

INFLUENCE OF PLATE WAVE CHARACTERISTICS ON THE ANGULAR DEPENDENCE OF ULTRASONIC VELOCITIES

R.B. Thompson, J.F. Smith, and S.S. Lee

Ames Laboratory
Iowa State University
Ames, IA 50011

INTRODUCTION

The angular dependence of the velocities of ultrasonic plane waves in a stressed, orthorhombic (orthotropic) continuum has recently been analyzed, and the results have been used to define scenarios for non-destructively measuring stress and preferred grain orientation [1,2]. These techniques make use of particular features which allow the two sources of anisotropy, stress and texture, to be separately determined. However, experimental realization of these ideas involves measurements at surfaces, and the influence of the surfaces on the plane wave solution must be considered. This paper treats the case of an orthorhombic plate, thin with respect to a wavelength. Discussions of the extensional and horizontal shear plate mode velocities appear in the mechanics literature, and their application to the characterization of the elastic constants of metal matrix composite plates has been investigated [3]. Here the theory is again briefly derived but in the previous notation [2] so as to allow the analytical expressions already obtained for the angular dependence of plane wave solutions to be directly compared to those for plate modes. Neglecting the effects of stress, the extent to which the S_0 (extensional or fundamental symmetric) and SH_0 (fundamental horizontally polarized shear) plate solutions differ from their plane wave L (longitudinal) and SH (horizontally polarized shear) counterparts are discussed. Application of the results to weakly anisotropic metal polycrystals indicates a substantial difference in the anisotropies of the S_0 and L solutions. Implication of the results to the ultrasonic measurement of preferred grain orientation (texture) in metal polycrystals is discussed.

THEORY

Consider a rolled plate, modeled as an orthorhombic continuum with the 1, 2, and 3-axis corresponding to the rolling, transverse, and thickness directions respectively. The stress σ_{ij} and strain ϵ_{kl} are related by the anisotropic generalization of Hooke's law, $\sigma_{ij} = C_{ijkl}\epsilon_{kl}$, where the elastic constant tensor C_{ijkl} has nine independent components and the strains are defined by $\epsilon_{kl} = (\partial u_k / \partial x_l + \partial u_l / \partial x_k) / 2$. The stress components σ_{13} must vanish at the surface of the plate and, at sufficiently small

thickness to wavelength ratios, can be neglected throughout the plate thickness. Consequently, $\epsilon_{23} = \epsilon_{13} = 0$ and $\epsilon_{33} = -(C_{13}\epsilon_{11} + C_{23}\epsilon_{22})/C_{33}$ (where the reduced elastic constant notation has been introduced). Solution of the equations of motion for the phase velocity V of straight crested waves propagating in the \vec{P} direction, leads to the secular equation

$$\begin{vmatrix} P_1^2 \hat{C}_{11} + P_2^2 C_{66} - \rho V^2 & P_1 P_2 (\hat{C}_{12} + C_{66}) \\ P_1 P_2 (\hat{C}_{12} + C_{66}) & P_1^2 C_{66} + P_2^2 \hat{C}_{22} - \rho V^2 \end{vmatrix} = 0, \quad (1)$$

where

$$\hat{C}_{11} = C_{11} - C_{13}^2/C_{33} \quad (2a)$$

$$\hat{C}_{12} = C_{12} - C_{13}C_{23}/C_{33} \quad (2b)$$

$$\hat{C}_{22} = C_{22} - C_{23}^2/C_{33}. \quad (2c)$$

Comparison to Eqs. (4) and (5) of Ref. 2 shows that, in the absence of stress, the secular equation for the plate modes at long wavelength is identical to that for plane waves if the elastic constants are redefined as in Eq. (2) above. The S_0 plate mode [4] becomes analogous to the quasi-longitudinal plane wave and the SH_0 plate mode [4] becomes analogous to the quasi-horizontally polarized plane shear wave. The flexural mode, which would be analogous to the vertically polarized plane shear wave, is not recovered since both its phase and group velocities vanish in this long wave length limit.

Equation (1) establishes that the functional form of the angular dependence of the long wavelength S_0 and SH_0 plate modes will be the same as that previously derived for plane waves [1,2]. To first order in the elastic anisotropy,

$$V_{S_0} = \left(\frac{\hat{C}_L}{\rho}\right)^{1/2} \left[1 + \frac{\hat{\alpha}}{4} \cos 2\theta - \left(\frac{\hat{\beta}\hat{C}_T}{4\hat{C}_L}\right) (1 - \cos 4\theta) + \dots\right] \quad (3a)$$

$$V_{SH_0} = \left(\frac{\hat{C}_T}{\rho}\right)^{1/2} \left[1 + \frac{\hat{\beta}}{4} (1 - \cos 4\theta) + \dots\right] \quad (3b)$$

where

$$\hat{C}_L = \left(\frac{C_{11} + C_{22}}{2}\right) - \left(\frac{C_{13}^2 + C_{23}^2}{2C_{33}}\right) \quad (4a)$$

$$\hat{C}_T = C_{66} \quad (4b)$$

$$\hat{\alpha} = [(C_{11} - C_{22}) - (C_{13}^2 - C_{23}^2)/C_{33}]/\hat{C}_L \quad (4c)$$

$$\hat{\beta} = \left\{ \left[\left(\frac{C_{11} + C_{22}}{2}\right) - C_{12} - 1/2 \frac{(C_{13} - C_{23})^2}{C_{33}} \right] / 2 - C_{66} \right\} / C_{66}. \quad (4d)$$

Analytical expressions for the terms to second order in the anisotropy, as well as the general solution, may be found in Ref. 2.

In Eq. (4), inclusion of only the terms involving C_{11} , C_{12} , C_{22} and C_{66} gives the corresponding parameters for plane wave propagation (\hat{C}_L , \hat{C}_T , $\hat{\alpha}$, $\hat{\beta}$).² The terms involving C_{13} , C_{23} , and C_{33} introduce the modifications due to the stress free surfaces of the plate. The average of the S_0 velocities for propagation in the 1 and 2 directions is $\sqrt{\hat{C}_L/\rho}$. The fact that this is slightly lower than the plane wave velocity average is a well known consequence of the plane stress character of the plate solutions as compared to the plane strain character of the plane wave solutions. Along the symmetry axes, the SH_0 velocities are identical to the plane wave values and are given by $\sqrt{\hat{C}_T/\rho}$. The parameters $\hat{\alpha}$ and $\hat{\beta}$ describe the anisotropy of the S_0 and SH_0 mode velocities, respectively. More specifically,

$$\hat{\alpha} = 2[v_{S_0}(0^\circ) - v_{S_0}(90^\circ)]/\sqrt{\hat{C}_L/\rho} \quad (5a)$$

$$\hat{\beta} = 2[v_{SH_0}(45^\circ) - v_{SH_0}(0^\circ)]/\sqrt{\hat{C}_T/\rho} \quad (5b)$$

From Eq. (4) it can be seen that both of these are modified from the plane wave values.

RELATIONSHIP TO POLYCRYSTALLINE ORIENTATION DISTRIBUTION

To quantify the differences in the plane wave and plate wave anisotropies, it is useful to introduce a model for the anisotropy of the elastic constants. For a polycrystal, the degree of preferred orientation of crystallites is often quantified by a crystallite orientation distribution function (CODF), $w(\xi, \psi, \phi)$, where the arguments are Euler angles describing the orientation of crystallites with respect to the sample axes [5]. It is often convenient to expand the CODF as a series of generalized Legendre functions, Z_{lmn} , as defined by Roe

$$w(\xi, \psi, \phi) = \sum_{l=0}^{\infty} \sum_{m=-l}^l \sum_{n=-l}^l W_{lmn} Z_{lmn}(\xi) e^{-im\psi} e^{-in\phi}. \quad (6)$$

For cubic crystallites, the lowest order independent coefficients are $W_{000} = 1/4 \sqrt{2} \pi^2$ (a normalization constant), and W_{400} , W_{420} , and W_{440} . Following the Voigt procedure for averaging elastic constants, the polycrystalline elastic constants of the orthorhombic plate may be expressed in terms of these four W_{lmn} coefficients and the single crystal elastic constants, C_{IJ}^0 . When the results are substituted into Eq. (4), one can then relate the experimentally observable parameters, \hat{C}_L , \hat{C}_T , $\hat{\alpha}$, and $\hat{\beta}$ to the W_{lmn} and C_{IJ}^0 . It is also convenient to define the isotropic Voigt average moduli $L = C_{11}^0 - 2C^0/5$, $P = C_{12}^0 + C^0/5$, and $T = C_{44}^0 + C^0/5$ where C^0 is the elastic anisotropy, $C^0 = C_{11}^0 - C_{12}^0 - 2C_{44}^0$. Then, to first order in the small parameters ($C^0 W_{lmn}/C_{IJ}^0$),

$$\hat{C}_L = C_L - [P^2 - \frac{32\sqrt{2}}{32} \pi^2 C^0 P(1+P/L)W_{400}]/L \quad (7a)$$

$$\hat{C}_T = C_T \quad (7b)$$

$$\hat{\alpha} = \alpha (1 + \frac{2P}{L}) / (1 - \frac{P^2}{L^2}) \quad (7c)$$

$$\hat{\beta} = \beta \quad (7d)$$

The parameters C_L , C_T , α and β , which govern the corresponding properties of the plane wave solutions, are given by

$$C_L = L + \frac{12\sqrt{2} \pi^2 C^0}{35} (W_{400} + \frac{\sqrt{70}}{3} W_{440}) \quad (8a)$$

$$C_T = T + \frac{4\sqrt{2} \pi^2 C^0}{35} (W_{400} - \sqrt{70} W_{440}) \quad (8b)$$

$$\alpha = \frac{-32\sqrt{5} \pi^2 C^0 W_{420}}{35 L} \quad (8c)$$

$$\beta = \frac{16\sqrt{35} \pi^2 C^0 W_{440}}{35 T} \quad (8d)$$

As noted before, \hat{C}_L is lower than C_L because of the reduced stiffness of the material in plane stress (plate mode) with respect to that in plane strain (plane wave). C_T is unchanged due to the lack of influence of the plate surfaces on horizontally polarized shear waves propagating in material symmetry directions. The S_0 mode anisotropy factor is considerably greater than the plane longitudinal wave anisotropy. For example, $\hat{\alpha} = 2.67\alpha$ when $P = L/2$. Thus the plate surfaces have a major influence on this parameter. To the order of this calculation, the SH_0 mode anisotropy is identical to that for plane waves, as is generally assumed in the literature [1,2,7]. Examination of Eq. (4d) indicates that differences between $\hat{\beta}$ and β exist to second order in the anisotropy $C^0 W_{lmn}/C^0_{IJ}$. These small differences occur because waves propagating along directions other than material symmetry axes are no longer purely shear in character and the dilational component is influenced by the stress free boundary condition at the plate surfaces.

The most striking difference between the plate and unbounded medium plane wave solutions is the increased anisotropy of the long wavelength S_0 mode solution with respect to that of the plane longitudinal wave. This can best be explained in the context of a numerical example. The case of aluminum has been selected; aluminum has single crystal elastic constants [8] (in GPa) of $C_{11}^0 = 108$, $C_{12}^0 = 62$, $C_{44}^0 = 28.3$, and $C^0 = -10.6$. The CODF coefficients have been taken to have the values $W_{400} = 0.001358$, $W_{420} = 0.000190$, and $W_{440} = -0.005590$ corresponding to a particular sample analyzed by Allen et al. [7] with neutron diffraction techniques. Table I presents the values of the parameters defined in Eqs. (7) and (8). The origin of the large difference between $\hat{\alpha}$ and α is illustrated in Fig. 1, in which the elastic constants contributing to these parameters are plotted as a function of W/W_{max} . It is assumed that the three W_{lmn} vary proportionally to one another from zero to the maximum values cited above.

Table. I. Wave Propagation Parameters for a Particular Aluminum Plate.

Plane Waves	Plate Waves
$C_L = 113.0$ GPa	$C_L = 80.9$ GPa
$C_T = 25.4$ GPa	$C_T = 25.4$ GPa
$\alpha = 0.000362$	$\alpha = 0.00105$
$\beta = 0.0604$	$\beta = 0.0604$

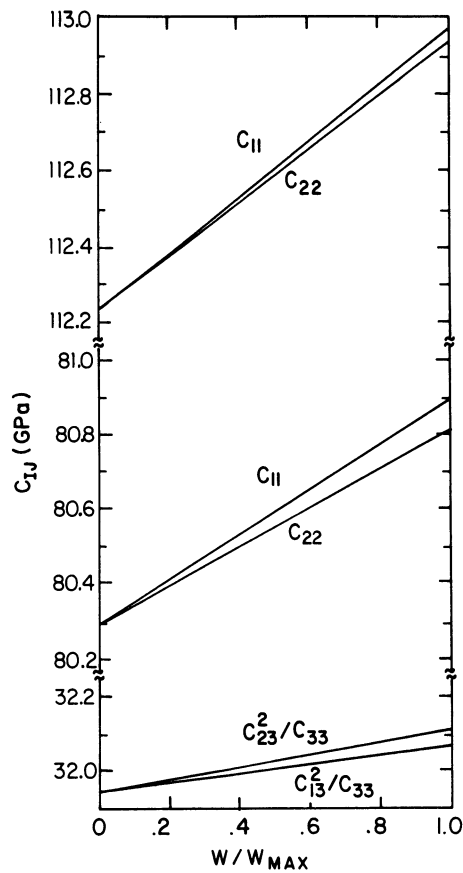


Fig. 1. Elastic constants influencing the plane and plate wave anisotropies of an aluminum polycrystal as a function of degree of texture.

From the graph, it can be seen that C_{11} increases faster than C_{22} while C_{13}^2/C_{33} increases slower than C_{23}^2/C_{33} , and hence the percentage difference between \hat{C}_{11} and \hat{C}_{22} are considerably greater than that between C_{11} and C_{22} .

The difference between the S_0 plate mode and plane wave solutions is illustrated by the plots of velocity versus angle in Fig. 2. These results correspond to a previously studied copper polycrystal ($C_{11}^0 = 169$, $C_{12}^0 = 122$, $C_{44}^0 = 75.3$, $C^0 = -103.6$, all in GPa) [8]. From the measured angular dependence of the velocities, Eqs. (7c), (7d), (8c) and (8d) imply $W_{420} = -1.66 \times 10^{-3}$ and $W_{440} = -1.22 \times 10^{-3}$. No data was available for evaluating W_{400} so this parameter was arbitrarily set equal to zero in the computation (the angular dependencies are insensitive to the particular values of W_{400} used). The angular dependence of the SH plane waves and SH_0 plate mode are identical to first order in the anisotropy. However the dramatic differences in the L-plane wave and S_0 plate mode angular dependences are clearly seen. As discussed above, $|V(90^\circ) - V(0^\circ)|$ is enhanced for the plate wave case.

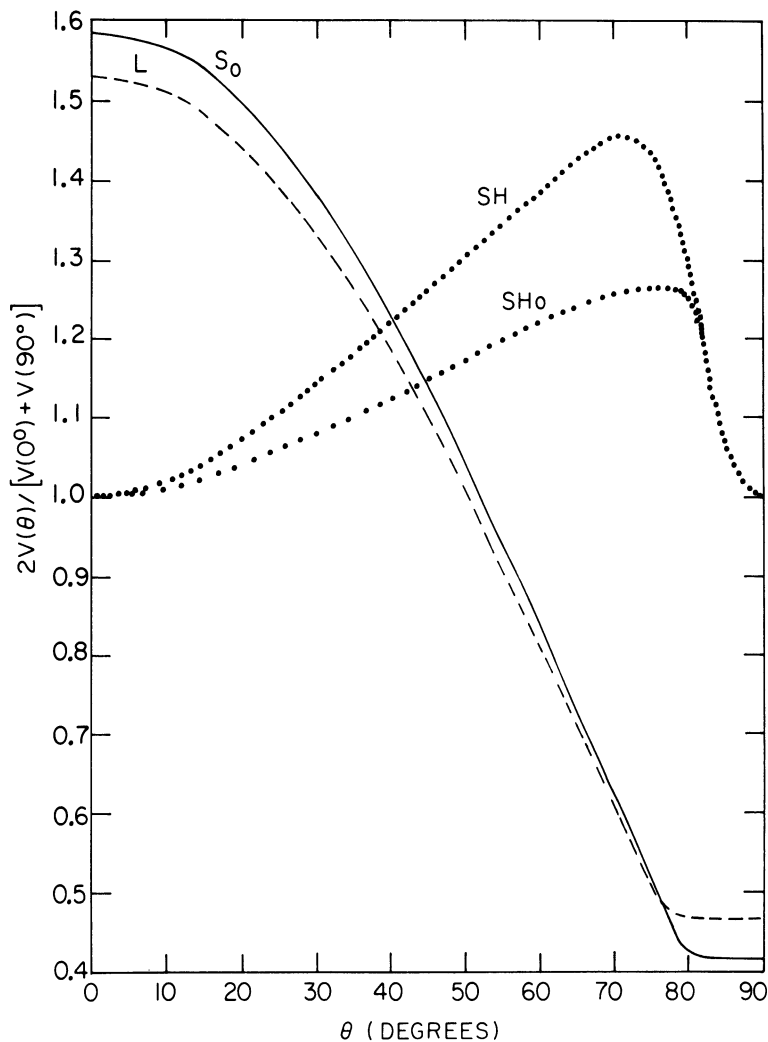


Fig. 2. Comparison of the normalized velocity of plane waves and plate modes for a copper polycrystal.

APPLICATION TO THE MEASUREMENT OF TEXTURE OF POLYCRYSTALS

Measurements of the long wavelength S_0 and SH_0 mode velocities and their angular dependence may be interpreted through Eqs. (7) and (8) to predict the coefficients W_{400} , W_{420} , and W_{440} in an expansion of the CODF [9]. These are sufficient to make a first order prediction of the result of x-ray or neutron pole figure analysis [5]. These ultrasonic pole figures will not contain all of the information of the full pole figures because of the absence of the higher order terms [10]. However, they may contain enough information for process control or quality assurance applications [11].

The theory suggests that the values of W_{420} and W_{440} determined from ultrasonic measurements will be quite accurate. However, difficulties may be encountered with determination of W_{400} because of the sensitivity to a) absolute velocity measurements and b) absolute errors in the formulae for polycrystal average elastic constants.

ACKNOWLEDGEMENT

This work was supported by U. S. Department of Energy, Office of Basic Energy Sciences, Division of Materials Sciences under contract no. W-7405-Eng-82.

REFERENCES

1. R. B. Thompson, J. F. Smith, and S. S. Lee, in NDE of Microstructure for Process Control, edited by H. N. G. Wadley (American Society of Metals, Metals Park, OH, 1985), pp. 73-80.
2. R. B. Thompson, S. S. Lee, and J. F. Smith, J. Acoust. Soc. Am., **80**, 921-931 (1986).
3. J. V. Foltz, A. L. Bertram, and C. W. Anderson, Report NSWC TR85-186 (Naval Surface Weapons Center, Dahlgren, Virginia, 1985).
4. B. A. Auld, Acoustic Waves and Fields in Solids (Wiley-Interscience, New York, 1973).
5. C. M. Sayers, J. Phys. D. **15**, 2157-2167 (1982).
6. R. J. Roe, J. Appl. Phys. **37**, 2069-2072 (1966).
7. D. R. Allen, R. Langmen, and C. M. Sayers, Ultrasonic **23**, 215-222 (1985).
8. R. F. S. Hearmon, Landolt-Börnstein, Numerical Data and Functional Relationships in Science and Technology, K.-H. Hellwege, Editor (Springer-Verlag, Berlin, 1979) Group III, Vol. 11, p. 9.
9. S. S. Lee, J. F. Smith and R. B. Thompson, "Inference of Crystallite Orientation Distribution Function from the Velocities of Ultrasonic Plate Modes," to be published in Proceedings of 2nd International Symposium on Nondestructive Characterization of Materials, J. F. Bussiere and J. P. Monchalin, Ed. (Plenum Press, New York, in press).
10. J. F. Smith, R. B. Thompson, D. K. Rehbein, T. J. Nagel, P. E. Armstrong, and D. T. Eash, "Illustration of Texture with Ultrasonic Pole Figures," in Review of Progress in Quantitative Nondestructive Evaluation, vol. 6, D. O. Thompson and D. E. Chimenti, Eds. (Plenum Press, New York, in press).
11. A. V. Clark, A. Govada, R. B. Thompson, G. V. Blessing, P. P. Del Santo, R. B. Mignogna, J. F. Smith and T. Nagel, "The Use of Ultrasonics for Texture Monitoring in Aluminum Alloys," *ibid.*